A Journal of the Gesellschaft Deutscher Chemiker

Angewandte International Edition GDCh Chemie

www.angewandte.org

Accepted Article

Title: Sulfur Poisoning and Self-Recovery of Single-Site Rh1/Porous Organic Polymer Catalysts for Olefin Hydroformylation

Authors: Siquan Feng, Miao Jiang, Xiangen Song, Panzhe Qiao, Li Yan, Yutong Cai, Bin Li, cunyao li, lili ning, Siyue Liu, Weiqing Zhang, Guorong Wu, Jiayue Yang, Wenrui Dong, Xueming Yang, Zheng Jiang, and Yunjie Ding

To be cited as: *Angew. Chem. Int. Ed.* **2023**, e202304282

Link to VoR: https://doi.org/10.1002/anie.202304282

WILEY VCH

10.1002/anie.202304282

WILEY-VCH

RESEARCH ARTICLE

Sulfur Poisoning and Self-Recovery of Single-Site Rh_1/Porous Organic Polymer Catalysts for Olefin Hydroformylation

Siquan Feng,[a]# Miao Jiang,[a]# Xiangen Song, # [a] Panzhe Qiao,[b] Li Yan,*[a] Yutong Cai,[a,d] Bin Li,[a,d] Cunyao Li,[a] Iili Ning,[a] Siyue Liu,[c] Weiqing Zhang,[c] Guorong Wu,[c] Jiayue Yang,[c] Wenrui Dong,*[c] Xueming Yang,[c,e] Zheng Jiang,[b] Yunjie Ding*[a,f]

[a] Dalian National Laboratory for Clean Energy, Dalian Institute of Chemical Physics, Chinese Academy of Sciences, 116023 Dalian, China. E-mail: Li Yan (yanli@dicp.ac.cn); Wenrui Dong (wrdong@dicp.ac.cn); Yunjie Ding (dyj@dicp.ac.cn).
[b] Shanghai Synchrotron Radiation Facility, Shanghai Institute of Applied Physics, and Shanghai Advanced Research Institute, Chinese Academy of Sciences, 201204 Shanghai, China.
[c] State Key Laboratory of Molecular Reaction Dynamics, Dalian Institute of Chemical Physics, Chinese Academy of Sciences, 116023, Dalian, China.
[d] University of Chinese Academy of Sciences, 100049 Beijing, China.
[e] Department of Chemistry, Southern University of Science and Technology, Shenzhen 518055, China.
[f] State Key Laboratory of Catalysis, Dalian Institute of Chemical Physics, Chinese Academy of Sciences, 116023 Dalian, China

Those authors contribute equally

* Correspondence: yanli@dicp.ac.cn (L.Y.), wrdong@dicp.ac.cn (W.D.), dyj@dicp.ac.cn (Y.D.)

Supporting information for this article is given via a link at the end of the document.

Abstract: Sulfur poisoning and regeneration are global deadly challenges for metal catalysts even at the ppm level. Fewer light was shed on the sulfur poisoning of single-metal-site catalysts and their regeneration. Herein, sulfur poisoning but self-recovery are first presented on an industrialized single-Rh-site catalyst (Rh_1/POPs). A decreased turnover frequency of Rh_1/POPs from 4317 h^{-1} to 318 h^{-1} was observed in a 1000 ppm H_2S co-feed for ethylene hydroformylation, but it self-recovered to 4527 h^{-1} after withdrawal of H_2S, while the rhodium nanoparticles demonstrated poor activity and self-recovery ability. H_2S reduced the charge density of the single Rh atom and lowered its Gibbs free energy with the formation of inactive $(SH)Rh(CO)(PPh_3\text{-frame})_2$, which could be regenerated to active $HRh(CO)(PPh_3\text{-frame})_2$ after withdrawing H_2S. The mechanism and the sulfur-related structure-activity relationship were highlighted. This work provides a forward understanding of the heterogeneous ethylene hydroformylation and the sulfur-poisoned regeneration in the catalysis science of single-atom catalysts.

Introduction

Sulfur poisoning of H_2S is a global and deadly challenge for metal nanoparticle catalysts, reducing the catalyst's activity and changing the product's selectivity even at the ppm level.[1] The sulfur species would adsorb strongly on the surface of metal nanoparticle catalysts, blocking the active sites and disrupting the reaction.[2] Besides, the formation of metal sulfide and the support sulfonation has also been reported as the factors leading to the sulfur poisoning of metal catalysts.[1a,1b,3] Regeneration of sulfur poisoning of metal catalysts hosts much intention no matter in the academy or industry.

There are many methods concerning this problem, such as increasing the temperature to decompose the sulfides and decrease the coverage of sulfur species,[4] employing alkaline metals to preferentially form sulfates,[5] introducing sulfating support like Al_2O_3 to prevent the formation of sulfur species,[6] using a method of P-doping to decrease the sulfur poisoning,[7] using an oxidation method to remove the sulfur species,[8] and employing a physical isolation strategy by constructing core-shell structure.[9] However, the regeneration of the sulfur poisoning is still energy-exhausting and far from satisfactory, because of the strong interaction of sulfur with the metal nanoparticle catalysts. Fewer light was shed on the sulfur poisoning and regeneration of single-metal-site catalysts (SMSCs), and the potential characteristic of self-recovery from sulfur poisoning. Therefore, despite the challenge of insight into the sulfur poisoning, regeneration, or self-recovery of SMSCs at the molecular level would gain much interest urgently.

The SMSCs, especially those with a mononuclear geometrical structure, are known for their versatile coordination ability and adjustability in electrical and geometrical structures.[10] In addition, the central metal ion of SMSCs often goes through a REDOX process during the reaction, accompanied by the earning and expense of valence electrons in the outermost shell. Interestingly, SMSCs generally could coordinate simultaneously with different kinds of ligands that contain -P, -N, -O, -S, -C, C=C, C≡C, and so on. Those ligands have surplus electrons while the central metal atom of SMSCs has vacant d orbitals.[11] The amazing point is that those ligands that coordinated with the central metal atom could react chemically with each other, such as migration insertion to make a new ligand, lowering the energy of the system to form a more stable configuration. A new product is subsequently produced via the reductive elimination of the newly formed ligand. There are many methods to implement this step, such as hydrogenolysis by H_2, alcoholysis by alcohols, hydrolysis by H_2O, ammonolysis by NH_3, and so on.

Sulfur species could also act as a ligand of SMSCs to react with the central metal ions, influencing their electronic density, lowering their Gibbs free energy, and affecting their activity and selectivity. While the sulfur species is a strong electron donor and could adsorb strongly on the surface of NPs, leading to severe sulfur poisoning. Therefore, the interactional difference of sulfur species on nanoparticles and SMSCs may demonstrate different results in catalysis.[12] The regeneration or self-recovery of the sulfur poisoning of SMSCs and NPs is supposed to be different.

10.1002/anie.202304282

The SMSCs have the potential to be self-recovered from sulfur poisoning, while it is difficult for NPs theoretically.

Olefins hydroformylation is a 100% atom-economical reaction to increase the carbon chain and produce a variety of aldehydes, alcohols, organic acids, and esters.[13] More than 20 million tons/year of aldehydes or alcohols were produced mainly with the homogeneous triphenylphosphine carbonyl rhodium $HRh(CO)(PPh_3)_3$ catalyst.[14] As an alternative to homogeneous catalysts, SMSCs are supposed to bridge the conceptual gap between homogeneous and heterogeneous catalysis.[15] Other biphephos or diphenylphosphino ligands are also used to adjust the coordination environment of the central Rh atoms.[16] In the 2020s, a 50,000 t/a facility of ethylene heterogeneous hydroformylation with a single-site Rh_1/POPs catalyst was realized in a fixed bed reactor by our team at Ningbo Juhua Co. Zhejiang, China (Figures S1 and S2).[17] So far, it has been in stable operation for more than two years. The total conversion rate of ethylene was 99.26%, the total conversion rate of propionaldehyde hydrogenation was 99.58%, and the selectivity of propionaldehyde and n-propanol was 99.51% and 98.64%, respectively. To the best of our knowledge, it may be the world's first industrial application of SMSCs. An interesting self-recovery from sulfur poisoning on this industrial single-site Rh_1/POPs catalyst was first observed, while it is poor on Rh nanoparticles. Therefore, it is of significance to address the problem and investigate the molecular reaction process, as well as the sulfur poisoning and the reversible self-recovery process.

In terms of the Rh_1/POPs catalyst, an ingeniously designed porous organic polymer (POPs) with a tri-4-vinyltriphenylphosphine (PPh_3) unit was prepared as a monomer, and then a polymer was fabricated as a carrier via solvothermal polymerization. The molecular structure of Rh_1/POPs was verified as $HRh(CO)(PPh_3\text{-frame})_3$, similar to that of homogeneous $HRh(CO)(PPh_3)_3$ catalyst. It is suggested that the abundant PPh_3 in POPs guaranteed the central metal ions a rich electron environment and higher heterogeneous activity than the corresponding homogeneous catalyst.[18] The evolutions of the molecular configuration of the Rh_1/POPs during the normal reaction, sulfur poisoning, and self-recovery were specifically and first addressed in this paper. Besides, as an excellent catalyst for hydrogen-atom exchange,[19] the reversible formation of the Rh-H and Rh-SH bond on Rh_1/POPs during temporary sulfur-poisoning and self-recovery was also highlighted. The sulfur-related metal-ligand interaction of Rh_1/POPs was first revealed from the viewpoint of electronics and geometrics. Characterizations of HAADF-STEM, EXAFS, MAS NMR, in-situ XPS, XANES, in-situ FEL TOF MS, in-situ TPD MS, and in-situ DRIFTS were implemented.

Results and Discussion

The Rh_1/POPs catalyst was prepared with simple impregnation of dicarbonyl rhodium (I) precursor on a porous organic polymer (POPs) support, which was synthesized via solvothermal polymerization with a tri-vinyl-triphenylphosphine monomer.[20] Meanwhile, the Rh nanoparticles catalyst on the POPs was prepared with divinylbenzene monomer (Rh/POPs-DVB). High-angle annular dark-field scanning transmission electron microscopy (HAADF-STEM) image suggested large amounts of Rh nanoparticles with the size of 1~2 nm (Figure 1a) on the support of the POPs-DVB, accompanied by part of scattering and isolated Rh atoms. Meanwhile, no nanoparticles could be discerned and the isolated metal atoms accommodated uniformly on the support of the POPs (Figure 1b). The phosphine ligand of the POPs should coordinate and immobilize the isolated Rh atoms. X-ray photoelectron spectroscopy (XPS) demonstrated an Rh $3d_{5/2}$ peak at the binding energy (B.E.) of 308.4 eV, which attributed to the positive Rh^+ electronic valence of Rh_1/POPs (Figure 1c), while the B.E. of the reference metal rhodium (Rh^0), oxide (Rh^{3+}) was 307.4 and 308.7 eV respectively. X-ray absorption near edge structure (XANES) of Rh_1/POPs further verified the Rh^+ electronic valence state of those isolated Rh atoms compared with the references of Rh foil (Rh^0) and Rh_2O_3 (Rh^{3+}) (Figure 1d). Extended X-ray absorption fine structure (EXAFS) was employed to confirm the first shell coordination environment of the isolated metal atoms of Rh_1/POPs. The EXAFS of Rh_1/POPs in R and the imaginary were processed (Figure 1d-1f), and it is clear to find that no bond of Rh-Rh existed in Rh_1/POPs, compared with the Rh foil reference. The bonding contribution analysis indicated a 1.0 coordination number of Rh-CO at 1.70 Å and a 3.0 coordination number of Rh-P at 2.22 Å for Rh_1/POPs (Figure 1g), indicating an $HRh(CO)(PPh_3\text{-frame})_3$ molecular structure of Rh_1/POPs (Figure 1h), which is analogous to the corresponding homogeneous $HRh(CO)(PPh_3)_3$ catalyst.[21] Therefore, it could be easy to realize the heterogenization of homogeneous catalysts by polymerizing ligands into porous organic support and then impregnating metal precursors.

The catalytic activity of Rh_1/POPs for ethylene hydroformylation was tested with the mixture gas of $CO/H_2/C_2H_4$ at 120 °C and 1.0 MPa in a fixed-bed reactor. A 1000-hour evaluation with a stable turnover frequency (TOF) of ~4300 h^{-1} was achieved in a normal feed of $CO/H_2/C_2H_4$ (1:1:1) at 120 °C and 1.0 MPa (Figure 2a). The severe sulfur poisoning of H_2S on the Rh_1/POPs was investigated in a feed containing 1000 ppm H_2S (denoted as H_2S co-feed) for ethylene hydroformylation. As indicated in Figure 2b and Table S1, Rh_1/POPs demonstrated a high TOF of 4317 $mol_{CO}/(mol_{Rh}•h)$ at the time on stream (TOS) of 16 hours in the normal feed, but it was feasibly sulfur poisoned to 229 h^{-1} during 3 hours after switching to 1000 ppm H_2S co-feed. The selectivity was free of effect and just a severe activity inhibition by H_2S happened on the Rh_1/POPs catalyst. Still, surprisingly the Rh_1/POPs could be self-recovered from sulfur poisoning just withdrawn the H_2S, and the TOF increased to 4527 h^{-1} during 8 hrs and stabilized at 4521 h^{-1} lastly in the normal feed. Meanwhile, the Rh nanoparticle supported on a POSs, which was prepared without the phosphine ligand but just with divinylbenzene monomer (Rh/POPs-DVB), was poor with the activity of 2.8 TOF at the TOS of 16 hours and was sulfur poisoned in H_2S co-feed (Figure 2c), and the sulfur-poisoning was hard to be recovered.

Besides, an expanded experiment of 1-octene hydroformylation was conducted within normal or H_2S co-feed to further confirm the general result for olefins hydroformylation. As indicated in Table S2, the Rh_1/POPs catalyst was poisoned with the conversion of 1-octene from 98.9% to 9.7% in a 1000 ppm H_2S co-feed, but it could also be self-recovered to 99.8% after the evacuation of H_2S and reaction in the normal feed. The temporary sulfur poisoning of H_2S and self-recovery was still achieved on the single-site Rh_1/POPs catalyst for olefins hydroformylation, which drew our attention to investigate the unique sulfur-related performance of Rh_1/POPs.

10.1002/anie.202304282

WILEY-VCH

RESEARCH ARTICLE

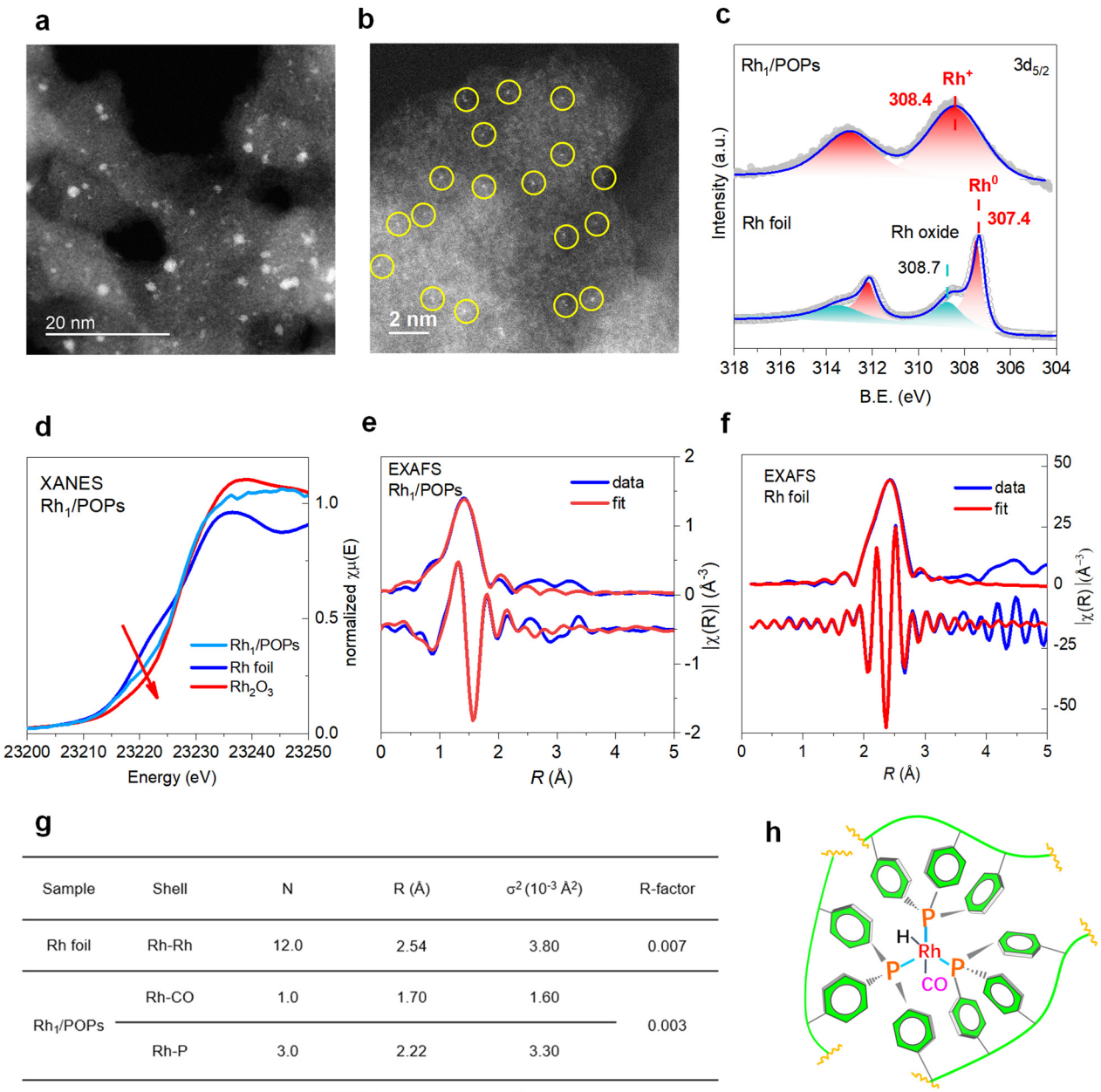

g

Sample	Shell	N	R (Å)	σ^2 (10^{-3} Å^2)	R-factor
Rh foil	Rh-Rh	12.0	2.54	3.80	0.007
Rh_1/POPs	Rh-CO	1.0	1.70	1.60	0.003
	Rh-P	3.0	2.22	3.30	

h

.**Figure 1.** Structure characterization of Rh_1/POPs and Rh/POPs-DVB. (a) HAADF-STEM image of Rh/POPs-DVB, (b) HAADF-STEM image of Rh_1/POPs, and (c) XPS of Rh_1/POPs. (d) XANES of Rh_1/POPs. (e) Rh EXAFS K-edge fitting of Rh_1/POPs in *R* space and imaginary part of Fourier transform. (f) Rh EXAFS K-edge fitting of Rh foil in *R* space and imaginary part of Fourier transform. (g) Quantitative analyses of Rh-Rh, Rh-CO, and Rh-P bond contributions in the first shell of Rh foil and Rh_1/POPs. *R* range: 1.0–3.0 Å; *k* range: 2.0–10.0 Å^{-1}; N, coordination number; R, the distance between absorber and backscatter; σ^2, Debye–Waller factor. (h) the molecular model of $HRh(CO)(PPh_3)_3$ of single-site Rh_1/POPs catalyst.

The reaction kinetics of ethylene hydroformylation on Rh_1/POPs were considered first. The reaction order of C_2H_4 and CO on Rh_1/POPs was 1.07 and 0.35 respectively, while it was 1.99 for H_2 (Figure 2d-2f), suggesting that the hydrogenolysis by H_2 was probably relevant to the rate-determining step leading to the sulfur-poisoning of Rh_1/POPs for ethylene hydroformylation. To further conjecture this supposition, a hydrogenation reaction of cyclohexene was executed with the same Rh_1/POPs catalyst. As shown in Table S3, the hydrogenation of cyclohexene was completely inhibited in the 1000 ppm H_2S co-feed, while a 67.2% conversion and 1149 h^{-1} TOF were achieved in the normal feed at very mild conditions (60 °C and 1.0 MPa). Therefore, the formation of Rh-H from H_2 hydrogenolysis on the Rh_1/POPs should be concerned well with the sulfur-poisoning of H_2S based on the result of olefins hydroformylation and hydrogenation. Two possible effects of sulfur poisoning could be deduced from the experimental data. The first one is that the adsorption dissociation of H_2 on Rh_1/POPs was difficult when the existence of H_2S, and another one is that the adsorption coordination of C_2H_4 or C_8H_{16} on Rh_1/POPs was difficult when the existence of H_2S.

10.1002/anie.202304282

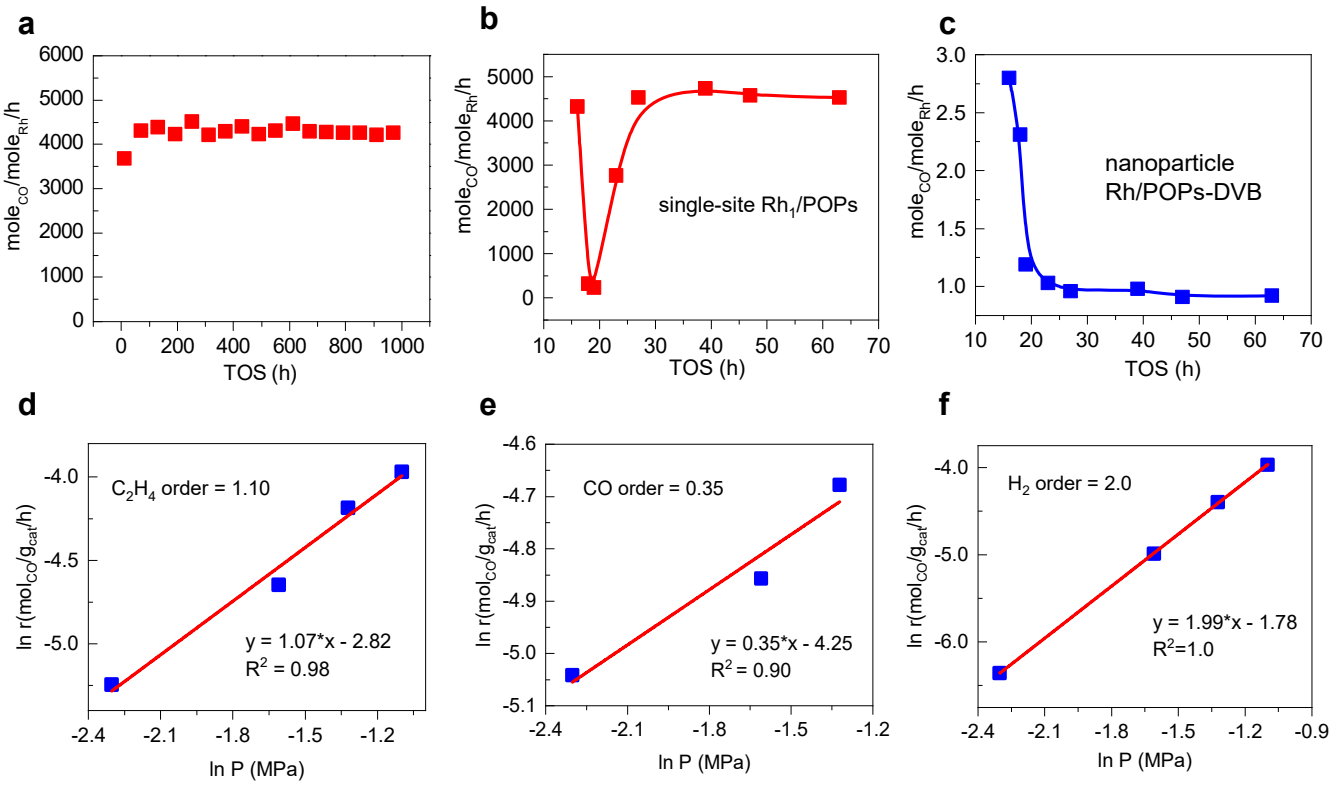

Figure 2. Activity test of single-site Rh_1/POPs and nanoparticle Rh/POPs-DVB catalysts. (a) Activity and stability test of Rh_1/POPs for ethylene hydroformylation. H_2S poisoning and recovery of (b) single-site Rh_1/POPs and (c) nanoparticle Rh/POPs-DVB catalysts for ethylene hydroformylation, and the 1000 ppm H_2S was introduced at TOS of 16 h and was withdrawn at TOS of 19 h. Conditions: Rh_1/POPs, Rh/POPs-DVB, 0.25wt%, 0.25g catalyst, 120°C, 1.0 MPa, C_2H_4:CO:H_2=1:1:1(with or without 1000 ppm H_2S), GHSV=4000 h^{-1}. Reaction order test of (d) C_2H_4, (e) CO, and (f) H_2 on Rh_1/POPs for ethylene hydroformylation.

To uncover the effect of H_2S on the geometrics of Rh_1/POPs, HAADF-STEM, EXAFS, MAS NMR, and wavelet transformation analysis are considered. It could be easy to find that the Rh atoms in the spent Rh_1/POPs were still isolated individually after the reaction no matter in normal or H_2S co-feed (Figure 3a-3c). The first shell coordination environment of those isolated Rh atoms was investigated (Figure S3), and no obvious Rh-Rh bond could be found no matter for the spent Rh_1/POPs in normal feed (denoted as Rh_1/POPs-R) or in H_2S co-feed (denoted as Rh_1/POPs-SR), or self-recovered from H_2S poisoning (denoted as Rh_1/POPs-SR-R) (Figure 3d-3f) when compared with the reference Rh foil (Figure 1f-1g). The wavelet transforms analysis also confirmed that the single Rh atoms were still isolated individually after reaction in normal or H_2S co-feed or self-recovery from sulfur-poisoning. Because the backscattered X-ray adsorption of Rh_1/POPs-R, Rh_1/POPs-SR, and Rh_1/POPs-SR-R was almost located at 5.0 Å and 1.7 Å in k and R space respectively, while it is 9.8 Å and 2.5 Å in k and R space for the reference Rh foil (Figure 3g-3i and Figure S4). Based on the above information, H_2S shouldn't agglomerate the single Rh atoms but probably affect their geometrical coordination structure, and consequently led to the sulfur poisoning of Rh_1/POPs. Besides, a bond of Rh-S is supposed to exit for Rh_1/POPs-SR.

EXAFS scattering path analysis suggested that the Rh_1/POPs-R was coordinated with an Rh-CO path at 2.09 Å and an Rh-P path at 2.33 Å, and their coordination numbers (CN) were 2.2 and 1.9, respectively (Table S4). The molecular model of Rh_1/POPs-R was anticipated as the pentacoordinate $HRh(CO)_2(PPh_3\text{-frame})_2$, which should originate from the active tetradentate species $HRh(CO)(PPh_3\text{-frame})_2$. While for the case of Rh_1/POPs-SR, the CN of Rh-CO and Rh-P was 1.0 and 2.9, respectively. In addition, a new Rh-S contribution at 2.46 Å with 1.2 CN could also be fitted for Rh_1/POPs-SR when compared with Rh_1/POPs-R. Thus, a pentacoordinate $(H_XS)Rh(CO)(PPh_3\text{-frame})_3$ (x=0, 1 or 2) was suspected for the molecular structure of Rh_1/POPs-SR, which may be originated from tetradentate species $(H_XS)Rh(CO)(PPh_3\text{-frame})_2$ (x=0, 1 or 2). For the case of Rh_1/POPs-SR-R, the CN of the Rh-P and Rh-CO was 2.5 and 2.0, respectively, similar to Rh_1/POPs-R, suggesting a process of self-recovery from sulfur poisoning.

Magic angle spinning nuclear magnetic resonance (MAS NMR) was employed to explore the geometrics of the Rh_1/POPs in sulfur poisoning and self-recovery. An increased chemical shift of δ(Rh-P) from 28.5 to 30.1 ppm that attributed to the coordination of PPh_3[22] was observed in sulfur poisoning of Rh_1/POPs (Figure S5a), which should be due to the bigger electronegativity of S (2.58) than P (2.19). While for the sulfur-poisoning recovery of Rh_1/POPs, a decreased chemical shift of δ(Rh-P) from 28.5 to 30.1 ppm was confirmed. Besides, the signal intensity at ~δ(28.5 ppm) corresponded well with the Rh-P coordination numbers (Table S4), which accorded well with the EXAFS results of Rh_1/POPs-R, Rh_1/POPs-SR, and Rh_1/POPs-R and further evidenced the self-recovery of Rh_1/POPs from sulfur poisoning.

10.1002/anie.202304282

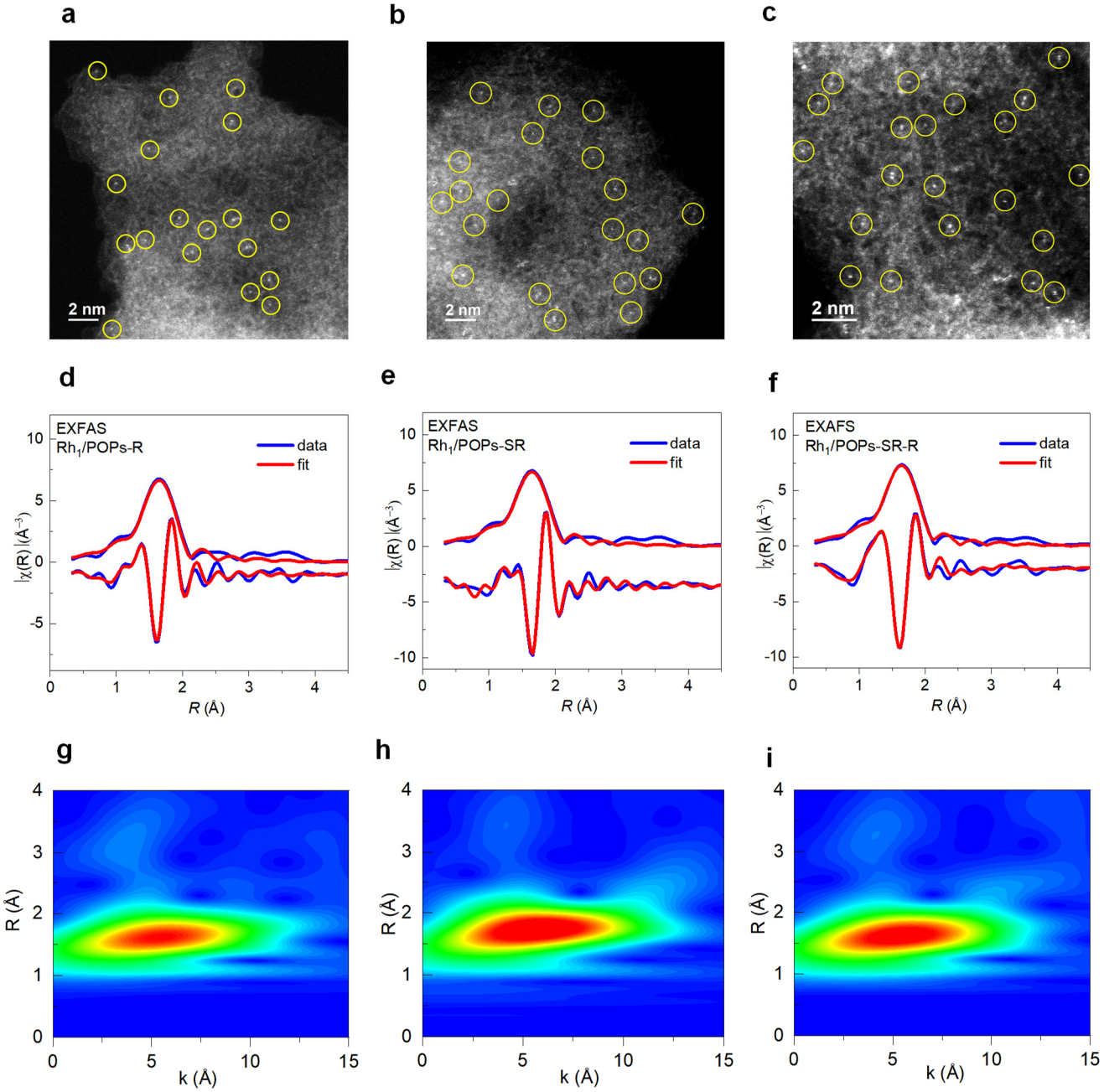

Figure 3. Geometric structure identification of Rh_1/POPs-R, Rh_1/POPs-SR and Rh_1/POPs-SR-R. HAADF-STEM image of (a) Rh_1/POPs-R, (b) Rh_1/POPs-SR, (c) Rh_1/POPs-SR-R; EXAFS fitting of (d) Rh_1/POPs-R, (e) Rh_1/POPs-SR, and (f) Rh_1/POPs-SR-R in *R* space and imaginary part of Fourier transform; the wavelet transform analysis of (g) Rh_1/POPs-R, (h) Rh_1/POPs-SR, (i) Rh_1/POPs-SR-R with k=2 weight. Rh_1/POPs-R, Rh_1/POPs-SR, and Rh_1/POPs-SR-R represent the spent Rh_1/POPs in normal feed, in 1000 ppm H_2S co-feed, and the spent Rh_1/POPs-SR in normal feed, respectively.

To figure out exactly the electronic effect of H_2S on the Rh_1/POPs catalyst, *in-situ* XPS experiments were implemented. For the process of sulfur poisoning, a severe electronic charge reduction happened to the isolated Rh atoms and the phosphine ligand of Rh_1/POPs in the H_2S co-feed. The B.E. of Rh $3d_{5/2}$ of Rh_1/POPs-SR was 307.3 eV, lower than that of the 308.1 eV in Rh_1/POPs-R (Figure 4a, Table S5), which may be due to the reduction characteristic of H_2S. The B.E. of $2P_{3/2}$ of Rh_1/POPs-SR was 130.9 eV, lower than that of the 131.3 eV in Rh_1/POPs-R as well (Figure 4b, Table S5), which may be related to the strong electronegativity effect of sulfur (S, 2.58; P, 2.19; Rh, 2.28).[23] Moreover, a new peak of P $2P_{3/2}$ formed at 129.3 eV, which should relate to the PPh_3 poisoned by H_2S.[24] Besides, a new peak of S $2P_{3/2}$ emerged at 161.7 eV for Rh_1/POPs-SR unexpectedly (Figure 4c, Table S5), which should ascribe to the coordinated sulfur species of [SH]/Rh (161.6 eV)[25] when compared with other alternative sulfur species, such as $(P(C_6H_5)_3)_2$-SH (162.0 eV),[26] $(S=P(C_6H_5)_3)$ (162.5 eV),[27] S (164.40 eV), Rh_2S_3 (163.4 eV) and H_2S 170.7 eV.[22a] U. Yoshio et al. also determined the adsorption dissociation of H_2S as [SH] on the Rh_xP catalyst during the hydrodesulfurization process.[22b] Therefore, sulfur poisoning of Rh_1/POPs suffered from severe electronic charge reduction with

10.1002/anie.202304282

the geometrical change of active HRh(CO)(P-frame)$_2$ to inactive (SH)Rh(CO)(P-frame)$_2$.

The Mulliken charge of HRh(CO)(P-frame)$_2$ and (SH)Rh(CO)(P-frame)$_2$ was also investigated theoretically with DFT. It is easy to find that [SH] coordination replaced [H] on the central Rh atom could indeed decrease the electronic charge from -0.364 to -0.453 (Figure 4d), which agreed well with the result of XPS. More importantly, the coordination of C_2H_4 on HRh(CO)(P-frame)$_2$ would increase the charge of the central Rh atom from -0.453 to -0.226 normally, while the coordination of C_2H_4 on (SH)Rh(CO)(P-frame)$_2$ decreased the charge of central Rh atom from -0.364 to -0.398 and simultaneously caused polarization of the charge of phosphine-containing ligands, and eventually led to sulfur poisoning of the Rh$_1$/POPs catalyst. The opposite effect of C_2H_4 coordination on these two kinds of central single Rh atoms demonstrated that C_2H_4 coordination is supposed to be difficult on (SH)Rh(CO)(P-frame)$_2$ when compared with HRh(CO)(P-frame)$_2$, which argued what we supposition before based on the reaction test results. The differential charge density of those two models further indicated that the difficult coordination of C_2H_4 on (SH)Rh(CO)(P-frame)$_2$ should result from the charge repulsion effect of [SH] (Figure 4d).

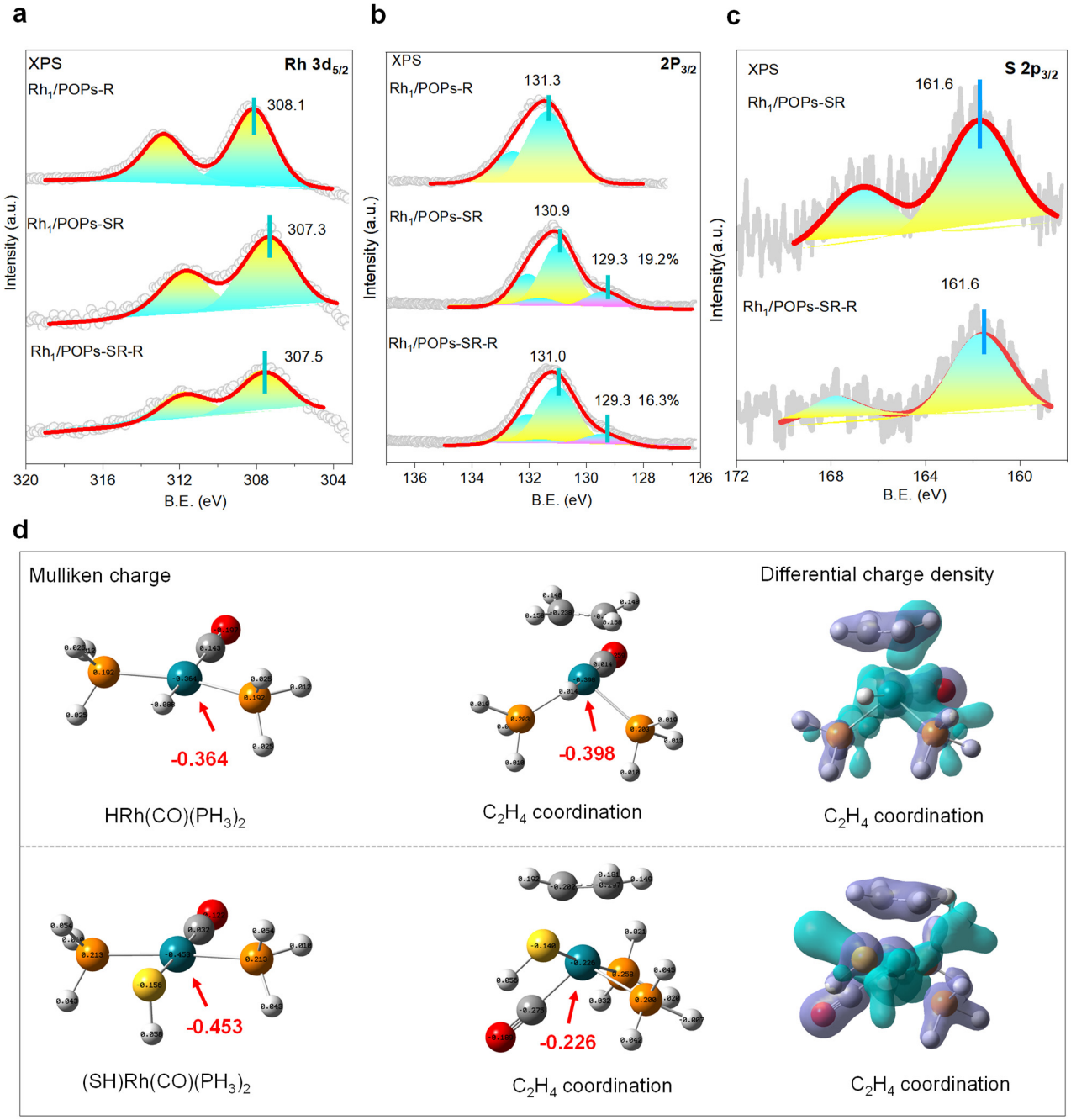

Figure 4. *In-situ* XPS of (a) Rh 3d$_{5/2}$, (b) P 2p$_{3/2}$, and (c) S 2p$_{3/2}$ of Rh$_1$/POPs spent in normal feed, in H_2S co-feed, or H_2S co-feed and then in normal feed. (d) The Muliken charge analysis and differential charge density analysis of the atoms of HRh(CO)(PH$_3$)$_2$ and (SH)Rh(CO)(PH$_3$)$_2$. For the differential charge density, the green areas are electron deficient and the brown areas are electron rich.

10.1002/anie.202304282

WILEY-VCH

RESEARCH ARTICLE

While for the self-recovery of Rh_1/POPs from sulfur poisoning, a recovery in electron valence was observed. *In-situ* XPS demonstrated a slight increase in B.E. of Rh $3d_{5/2}$ from 307.3 eV to 307.5 eV (Figure 4a, Table S5). The ratio of the sulfur-poisoned P $2p_{3/2}$ at 129.3 eV decreased from 19.2% to 16.3% (Figure 4b, Table S5). The integral area of the S $2p_{3/2}$ became smaller as well (Figure 4c, Table S5), suggesting the reversibility of sulfur poisoning of Rh_1/POPs by H_2S. *Ex-situ* XPS also exhibited a more pronounced increase in the binding energy of Rh $3d_{5/2}$ from 306.9 to 307.2 eV during the process of self-recovery (Figure S6a, Table S6). And unexpectedly, the sulfur-poisoned P $2p_{5/2}$ at 129.2 eV and the newly formed S $2p_{3/2}$ at 160.9 eV in Rh_1/POPs-SR disappeared after the withdrawal of H_2S (Figure S6b and S6c, Table S6), suggesting the self-recovery feasibility from sulfur poisoning of Rh_1/POPs in real reaction conditions. Therefore, although a strong electronegativity effect of sulfur poisoning was observed, the Rh_1/POPs-SR could be self-recovered under the normal reaction condition after the withdrawal of H_2S. In addition, the formation of the Rh-SH bond in Rh_1/POPs-SR and the fading of the Rh-SH bond in Rh_1/POPs-SR-R witnessed the sulfur poisoning and self-recovery of Rh_1/POPs.

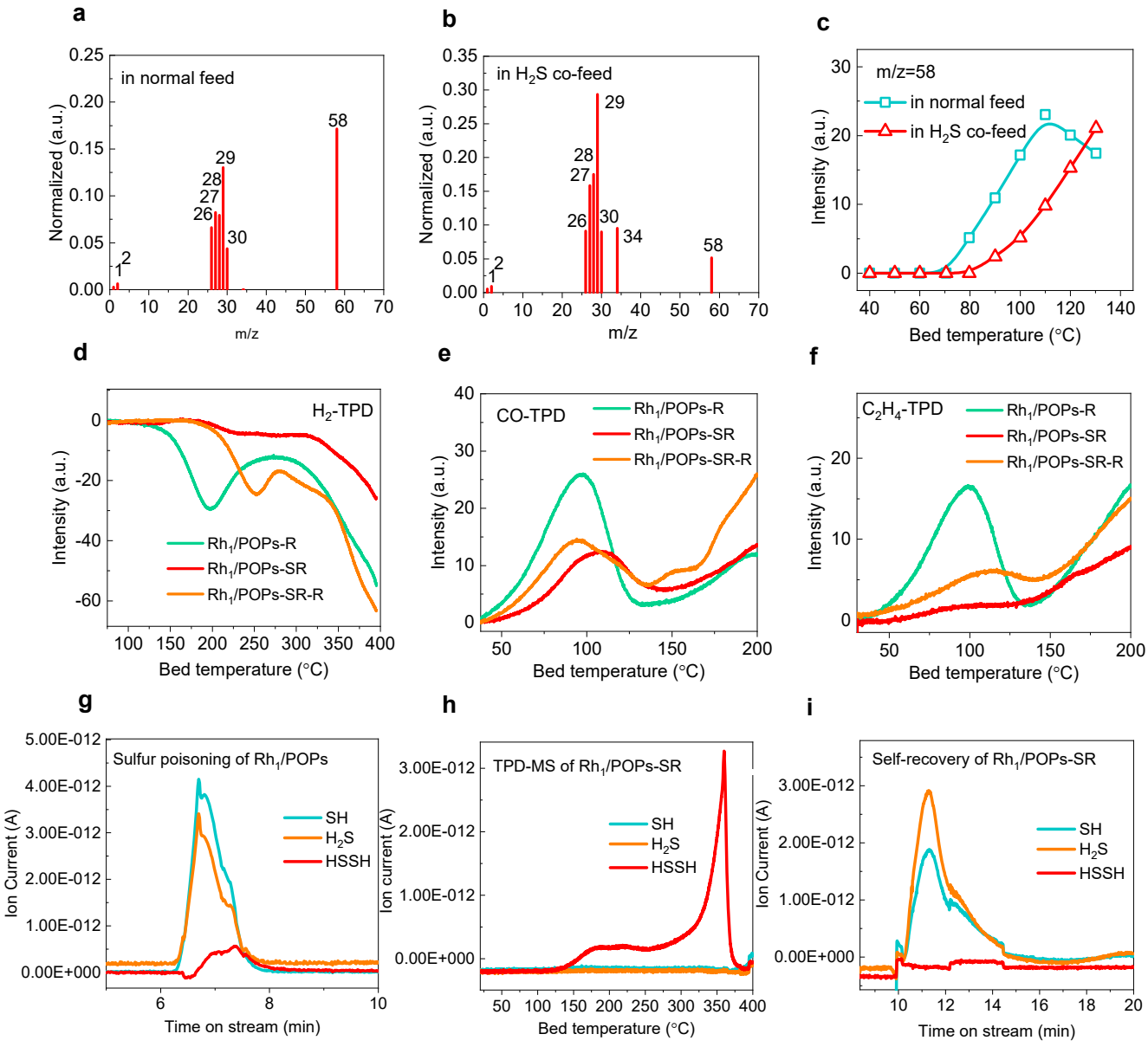

Figure 5. In-situ FEL TOF-MS of Rh_1/POPs for ethylene hydroformylation reaction (a) in the normal or the (b) H_2S co-feed at 100 °C. (c) The normalized in-situ FEL TOF-MS signal intensity of m/z=58 on Rh_1/POPs in the normal feed or H_2S co-feed with the bed temperature function, Free electron laser: 115 nm, 17.5uJ, energy fluctuations 25%, signal amplification x 25. In-situ (d) CO-TPD, (e) H_2-TPD, and (f) C_2H_4-TPD signals of Rh_1/POPs-R, Rh_1/POPs-SR, and Rh_1/POPs-SR-R. (g) In-situ MS signals of sulfur species (H_2S, SH, HSSH) in the sulfur poisoning of Rh_1/POPs in H_2S co-feed, (h) TPD-MS signals of sulfur species (H_2S, SH, HSSH) of Rh_1/POPs-SR, and (i) in-situ MS signals of sulfur species (H_2S, SH, HSSH) of Rh_1/POPs-SR in the process of self-recovery for ethylene hydroformylation in normal feed.

10.1002/anie.202304282

The structure evolution of the single-site Rh_1/POPs at the molecular level was addressed with the exchange of different reactants as ligands. As mentioned above, the Rh_1/POPs with the initial molecular structure of $HRh(CO)(PPh_3\text{-frame})_3$, which could activate under the reduction of CO/H_2 and transform to $HRh(CO)_2(PPh_3\text{-frame})_2$ or $HRh(CO)(PPh_3\text{-frame})_2$. For the normal reaction of ethylene hydroformylation in homogeneous $HRh(CO)(PH_3)_2$, it was generally acknowledged that the mechanism includes the following elementary steps of 1) C_2H_4 coordination as $H(C_2H_4)Rh(CO)(PPh_3)_2$, 2) C_2H_4 alkylation to form C_2H_5 as $(C_2H_5)Rh(CO)_2(PPh_3)_2$, 3) CO migration insertion to form C_2H_5CO as $(C_2H_5CO)Rh(CO)(PPh_3)_2$, 4) H_2 adsorption coordination, and 5) C_2H_5CO hydrogenolysis to produce C_2H_5CHO (Figure S7) and regenerate $HRh(CO)(PPh_3)_2$. Wilkinson et al pointed out that the hydrogenolysis of C_2H_5CO by H_2 is the rate-determining step on homogeneous $HRh(CO)(PPh_3)_2$ catalyst. [23a,28] Garland et al also observed a rhodium-acyl intermediate of $(C_2H_5CO)Rh(CO)(PPh_3)_2$ as the resting state of the catalyst using in-situ IR spectroscopy.[29] ^{13}C cross-polarization magic angle spinning nuclear magnetic resonance (^{13}C CP/MAS NMR) of Rh_1/POPs-SR showed two obvious peaks at δ(10.4 ppm) and δ(27.8 ppm), which was attributed to the sp^3 carbon of $–CH_3$ and $–CH_2–$ respectively (Figure S5b).[30] Thus, the sulfur poisoning of Rh_1/POPs should happen after the step of CO migrated insertion and before the step of CH_3CH_2CO reductive elimination by H_2, which further validated our previous speculation concerning the sulfur poisoning of Rh_1/POPs in the step of the adsorption coordination of H_2. As result, inactive sulfur poisoned species $(SH)Rh(CO)(PPh_3)_2$, $(SH)Rh(CO)_2(PPh_3)_2$, and $(SH)Rh(CO)(PPh_3)_3$ would be produced. However, it could be transformed into active $HRh(CO)(PPh_3)_2$ during the self-recovery process after the withdrawal of H_2S.

To further investigate the structural evolution of the single-site Rh_1/POPs at the process of H_2S poisoning, *in-situ* free-electron laser time of flight mass spectrometry (*in-situ* FEL-TOF/MS) was implemented at the Dalian Coherent Light Source of China.[31] The single-photon energy of the laser was 10.78 eV, which could ionize the reactants C_2H_4 (m/z=28), the toxic H_2S (m/z=34), and the product C_2H_5CHO (m/z=58), and their ionization energy was 10.51, 10.46, and 9.96 eV, respectively (Table S7). Normally, the product C_2H_5CHO (m/z=58) signal increased while the reactant C_2H_4 (m/z=28) signal weakened (Figure 5a). However, the signal of C_2H_5CHO (m/z=58) was dramatically inhibited and a stronger signal of C_2H_4 (m/z=28) was observed for Rh_1/POPs in the H_2S co-feed (Figure 5b), indicating a severe sulfur poisoning of Rh_1/POPs by H_2S, which agreed well with the catalytic activity of Rh_1/POPs reaction in normal feed or H_2S co-feed. Temperature function evolution demonstrated that the formation of C_2H_5CHO was inhibited in the H_2S co-feed (Figure 5c). Intriguingly, the signal of C_2H_5 (m/z=29) increased significantly in the H_2S co-feed, almost two times that in the normal feed (Figure 5a and 5b), implying that H_2S indeed correlated with the hydrogenolysis of C_2H_5CO on Rh_1/POPs for ethylene hydroformylation.

Besides, the *in-situ* temperature program desorption (*in-situ* TPD) was also implemented to further investigate the sulfur effect on Rh_1/POPs for ethylene hydroformylation. The adsorptions of H_2, CO, and C_2H_4 on Rh_1/POPs-SR were inhibited to some extent inordinately (Figure 5d-5f). Especially, the coordination of H_2 and C_2H_4 on Rh_1/POPs-SR was almost completely suppressed in the H_2S co-feed, it should be related to the sulfur poisoning of Rh_1/POPs. However, the TPD signals of H_2, CO, and C_2H_4 on Rh_1/POPs-SR-R demonstrated a degree of self-recovery from sulfur poisoning, indicating the self-recovery of Rh_1/POPs-SR after the withdrawal of H_2S. Besides, the *in-situ* TPD mass spectrums of sulfur species in the process of sulfur poisoning and self-recovery were also emphatically considered. H_2S was transferred into SH in the process of sulfur poisoning (Figure 5g), but it coupled easily as a dimer of HSSH in a higher temperature above 120°C, and no SH and H_2S signals were detected (Figure 5h). Meanwhile, only the species of SH and H_2S were detected in the self-recovery process of Rh_1/POPs-SR (Figure 5i).

Therefore, the sulfur poisoning of Rh_1/POPs by H_2S should happen concerning the $(C_2H_5CO)Rh(CO)(PPh_3\text{-frame})_2$ hydrogenolysis, followed by the formation of inactive $(SH)Rh(CO)(PPh_3\text{-frame})_2$, on which the adsorption coordination of H_2 and C_2H_4 was difficult when compared with the normal $HRh(CO)(PPh_3\text{-frame})_2$. $(SH)Rh(CO)(PPh_3\text{-frame})_2$ then reasonably transformed to $(SH)Rh(CO)(PPh_3\text{-frame})_3$ and $(SH)Rh(CO)_2(PPh_3\text{-frame})_2$ after reaction. Nevertheless, those inactive sulfur-related species could transform into active $HRh(CO)(PPh_3\text{-frame})_2$ by CO/H_2 after withdrawal of H_2S thanks to their potential in activation of H_2 and the amiable metal-ligand interaction of mononuclear complex.

To insight into the structural evolution of Rh_1/POPs in sulfur poisoning and self-recovery for ethylene hydroformylation, *in-situ* diffuse reflectance Fourier infrared spectroscopy (*in-situ* DRFIRS) was conducted. As indicated in Figure 6a and Figure S8, the absorption peaks at 948 and 1735 cm^{-1} were attributed to the surface distortion vibration of ν(C-H) of C_2H_4 and the stretching vibration of ν(C=O) of the product C_2H_5CHO, respectively. Besides, the peaks at 1947 and 2001 cm^{-1} were ascribed to the symmetric and asymmetric stretching vibration peaks of (Rh-CO),[19] and most critically the peak at 2045 cm^{-1} was attributed to the stretching vibration of ν(Rh-H) in $HRh(CO)_2(PPh_3\text{-frame})_2$.[19,32] The reference sample of $HRh(CO)(PPh_3)_3$ also confirmed the two peaks at 1923 and 2038 cm^{-1}, which were assigned to ν(Rh-CO) and ν(Rh-H), respectively.[32] Normally, the growth of ν(C=O) at 1735 cm^{-1} and the strengthening of ν(Rh-CO) at 1947 and 2001 cm^{-1} with time on stream suggested the molecular evolution of Rh_1/POPs as $(C_2H_5CO)Rh(CO)(PPh_3\text{-frame})_2$ and $HRh(CO)_2(PPh_3\text{-frame})_2$, respectively (Figure 6a). In addition, the peak evolution at 2717 and 2812 cm^{-1} that belonged to the bending vibration and stretching vibration of ν(C=O) consistent with the ν(C=O) peak evolution of the C_2H_5CHO product. The affiliations of other peaks were attached in the supporting information (Table S8). It could be easy to find that the ν(Rh-CO), ν(Rh-H), and the ν(C=O) peaks increased quickly as time goes on for the Rh_1/POPs in normal feed, while the ν(C=O) of C_2H_5CO increased accordingly, suggesting the normal ethylene hydroformylation on Rh_1/POPs.

In terms of the sulfur poisoning of Rh_1/POPs in H_2S co-feed, the C_2H_4 adsorption (948 cm^{-1}) and the ν(C=O) vibration signals decreased dramatically (1735, 2715, and 2815 cm^{-1}) with time on stream (Figure 6b), in comparison with that in normal feed. More importantly, new peaks at 2065 and 1960 cm^{-1} increased while the peaks at 1984 and 2039 cm^{-1} attenuated, suggesting the transformation of active species into inactive species by H_2S. The

10.1002/anie.202304282

peak at 1984 cm^{-1} was assigned to the ν(C=O) of $(C_2H_5CO)Rh(CO)(PPh_3\text{-frame})_2$, while the peaks at 2065 and 1960 cm^{-1} were attributed to the ν(C=O) of inactive species $(HS)Rh(CO)_2(PPh_3\text{-frame})_2$. And critically, the ν(Rh-H) at 2039 cm^{-1} vanished in the H_2S co-feed (Figure 6b).

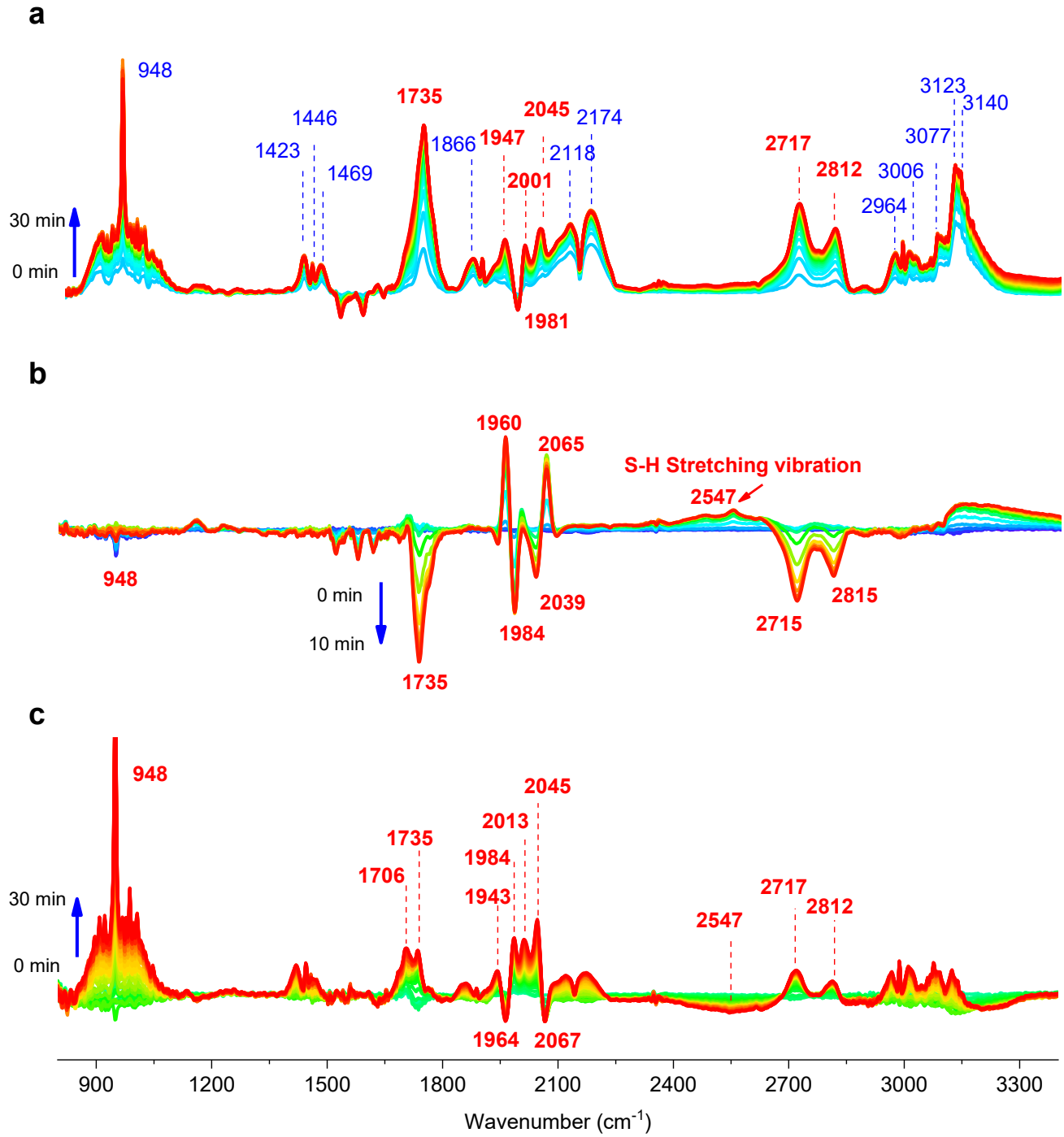

Figure 6. *In-situ* time-resolved DRFTIR spectroscopy of Rh_1/POPs for ethylene hydroformylation. (a) Rh_1/POPs reaction in normal feed, (b) Rh_1/POPs reaction in 1000 ppm H_2S co-feed, (c) Rh_1/POPs-SR reaction in normal feed, Conditions: 120°C, 101 KPa, $CO/H_2/C_2H_4$=1:1:1, the mass flowmeter 20 ml/min.

Meanwhile, a stretching vibration peak of ν(S-H) at 2547 cm^{-1} emerged. Therefore, the sulfur poisoning of Rh_1/POPs by H_2S should happen on the tetra-dentate unsaturated $(C_2H_5CO)Rh(CO)(PPh_3\text{-frame})_2$ to occupy part of the vacant space and then be revolutionized as $(SH)Rh(CO)(PPh_3\text{-frame})_2$. It could lastly be revolutionized as $(SH)Rh(CO)_2(PPh_3\text{-frame})_2$ and $(SH)Rh(CO)(PPh_3\text{-frame})_3$ in the process of cooling down. As a contrast, the hydrogenolysis of $(C_2H_5CO)Rh(CO)(H_2)(PPh_3\text{-frame})_2$ by H_2 fulfilled the formation of $HRh(CO)(P\text{-frame})_2$ in the normal feed. Therefore, sulfur poisoning not only led to a dramatic reduction of electronic charge valence of the central Rh atoms

10.1002/anie.202304282

electronically but also revolutionized it as inactive (SH)Rh(CO)(PPh$_3$-frame)$_2$ geometrically,[28] which severely inhibited the adsorption coordination of C_2H_4 and subsequently suppressed the reaction.

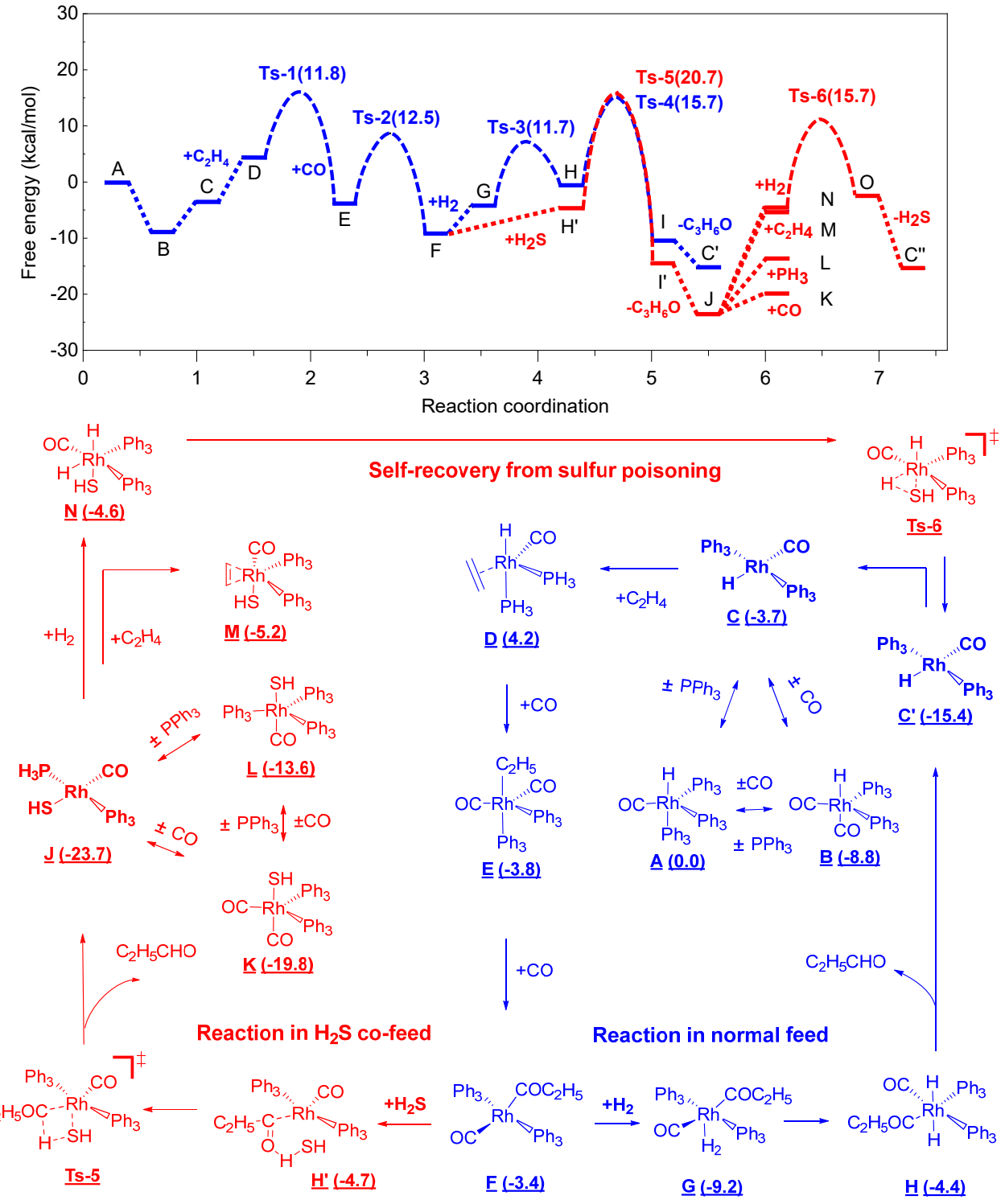

Figure 7. The DFT calculated the relative Gibbs free energy of H_2S poisoning and self-recovery of single-site Rh_1/POPs based on the proposed process of ethylene hydroformylation. (Energy unit: kcal/mol).

Nevertheless, the sulfur poisoning of Rh_1/POPs was not permanent, and the sulfur-poisoned Rh_1/POPs-SR could transfer into active species and realize the self-recovery just the withdrawal of H_2S. Correspondingly, the (Rh-CO) peaks of (HS)Rh(CO)$_2$(PPh$_3$-frame)$_2$ at 2067 and 1964 cm^{-1} disappeared gradually with time on stream during the process of self-recovery (Figure 6c), clearly witnessing the case of the self-recovery of Rh_1/POPs-SR after the withdrawal of H_2S. Meanwhile, the peaks of ν(Rh-CO) (1943 and 2013 cm^{-1}) increased, suggesting the restored formation of active species HRh(CO)$_2$(PPh$_3$-frame)$_2$.

10.1002/anie.202304282

Moreover, $(CH_3CO)Rh(CO)(PPh_3\text{-frame})_3$ (1984 cm^{-1}) was regenerated once again. Comparatively, the ν(S-H) at 2547 cm^{-1} faded, and the adsorption of the C_2H_4 peak at 948 cm^{-1} self-recovered. As a result, the related peaks of C_2H_5CO at 1735, 2717, and 2812 cm^{-1} reappeared. Besides, the peak of ν(Rh-H) at 2045 cm^{-1} reformed probably due to the structural evolution of $(HS)Rh(CO)_2(PPh_3\text{-frame})_2$ to $HRh(CO)_2(PPh_3\text{-frame})_2$ after the withdrawal of H_2S, further confirmed the amiable metal-ligand interaction of mononuclear catalysts. Therefore, sulfur poisoning and self-recovery of Rh_1/POPs include an interesting electronic effect but also embody a molecular structure evolution, as well as the formation and fading of Rh-SH bond in ethylene hydroformylation.

To elucidate the theoretical mechanism of Rh_1/POPs in sulfur poisoning and self-recovery, a reaction process of ethylene hydroformylation was proposed based on DFT calculation in Figure 7 and Figure S9, referring to the dissociation mechanism of $HRh(CO)(PPh_3)_3$ in a homogeneous system (Figure S7).[33] Gibbs free energy of the molecular models of Rh_1/POPs was calculated, and the frame of PPh_3 was simplified as PH_3. Normally, the active (**C**) $HRh(CO)(PH_3)_2$ originated from (**A**) $HRh(CO)(PH_3)_3$ or (**B**) $HRh(CO)_2(PH_3)_2$ via the syngas treatment (Figure 7 and Figure S9), followed by the formation of (**D**) $HRh(C_2H_4)(CO)(PH_3)_2$ due to the CO dissociation and C_2H_4 coordination. Subsequently, hydride alkylation with the energy barrier of 11.8 kcal/mol (**Ts-1**) for the formation of (**E**) $(C_2H_5)Rh(CO)_2(PH_3)_2$, and then a rhodium-acyl complex (**F**) $(C_2H_5CO)Rh(CO)(PH)_2$ was regenerated through CO insertion, and the Gibbs free energy barrier is 12.5 kcal/mol (**Ts-2**). The unsaturated rhodium-acyl complex (**F**) then underwent adsorption dissociation of H_2 to form (**G**) $(C_2H_5CO)Rh(H_2)(CO)(PH_3)_2$ and (**H**) $(C_2H_5CO)Rh(H)_2(CO)(PH_3)_2$, and then hydrogenolysis of C_2H_5CO fulfilled the catalytic cycle with the Gibbs free energy barrier of 11.7 and 15.7 kcal/mol, respectively, accompanied by the regeneration of (**C'**) $HRh(CO)_2(PH_3)_2$ and the production of C_2H_5CHO.

Among which, hydrogenolysis of (**G**) $(C_2H_5CO)Rh(H)_2(CO)(PH)_2$ was the rate-determining step with the highest energy barrier, which provided an opportunity for H_2S to competitive coordination as a special (**H'**) $(C_2H_5COHSH)Rh(CO)(PH_3)_2$, which subsequently turned into (**J**) $(SH)Rh(CO)(PH_3)_2$, (**K**) $(SH)Rh(CO)_2(PH_3)_2$, and (**L**) $(SH)Rh(CO)(PH_3)_3$ (Figure 7). Notably, the structure $(C_2H_5CO)(SH_2)Rh(CO)(PH_3)_2$ couldn't exist even though a large number of trial and error in DFT calculation, or the $(C_2H_5COHSH)Rh(PH_3)_2$ structure is more preferential or spontaneously produced. Among these geometrics, (**J**) $(SH)Rh(CO)(PH_3)_2$ possessed the lowest relative Gibbs free energy (-23.7 kcal/mol), while the Gibbs free of $HRh(CO)(PH_3)_2$ is only -15.4 kcal/mol. The species with lower Gibbs free energy tend to be privileged formed, and more stable in thermodynamically. Therefore, the sulfur poisoning of Rh_1/POPs by H_2S is much more favorable. For the case of (**J**) $(SH)Rh(CO)(PH_3)_2$, C_2H_4 and H_2 were very difficult to coordinate with the central Rh atoms (Figure 7 and Figure S9), and it got over the energy of 18.5 kcal/mol and 19.1 kcal/mol, respectively. Nevertheless, the sulfur poisoning of Rh_1/POPs could be self-recovered after the withdrawal of H_2S thanks to the amiable metal-ligand interaction and their potential for activation of H_2. The sulfur-related inactive $(SH)Rh(CO)(PH_3)_2$ could be revolutionized as active $HRh(CO)(PH_3)_2$ by CO/H_2, and the transition state Gibbs frees energy barrier was just 15.7 kcal/mol (Figure 7 and Figure S10), certificating the availability of self-recovery in theoretically.

Conclusion

In a word, temporary sulfur poisoning and the self-recovery problem of single-site Rh_1/POPs by H_2S were addressed in ethylene heterogeneous hydroformylation. H_2S severely inhibited the activity of Rh_1/POPs at a ppm level, but it could be self-recovered after withdrawing H_2S, while it is not for Rh nanoparticle. The rate-determining step of the hydrogenolysis of $(C_2H_5CO)Rh(CO)(PPh_3\text{-frame})_2$ provided an opportunity for H_2S to vicious competition with H_2 coordination. H_2S coordination revolutionized Rh_1/POPs as $(SH)Rh(CO)(PPh_3\text{-frame})_2$, which possessed the lowest Gibbs energy and C_2H_4 failed to coordinate because of the high Gibbs free energy barrier, and subsequently led to the sulfur poisoning of Rh_1/POPs in H_2S co-feed. However, the sulfur poisoning of Rh_1/POPs could be self-recovered after the withdrawal of H_2S. Besides, the Rh-SH from the dissociation of H_2S inhibited the coordination of C_2H_4 via the electronic repulsion effect. However, the Rh-SH was vulnerable and the SH could be eliminated as H_2S by CO/H_2 in the process of self-recovery. The inactive $(SH)Rh(CO)(PPh_3\text{-frame})_2$ could evolve as the active $HRh(CO)(PPh_3\text{-frame})_2$ just in the normal feed without any action. This work benefits understanding the structure-activity relationship of ethylene hydroformylation on single-Rh-site from the viewpoint of electrics and geometrics and is promising to open a door to developing sulfur-related chemistry concerning the sulfur poisoning and self-reversibility of single-metal-site catalysts.

Acknowledgments

The financial support for this work by the National Natural Science Foundation of China (22002156, 22108275, and 22108276, 22288201), the Youth Innovation Promotion Association of the Chinese Academy of Sciences (2022179, 2021181), the Innovation fund of DICP I202237, the CAS Project for Young Scientists in Basic Research (YSBR-022), the Strategic Priority Research Program of the Chinese Academy of Sciences (No. XDA21020300, No. XDB17020400, and No. XDA29040400), the international partnership program of the Chinese Academy of Sciences (No. 121421KYSB20170012), the Key Technology Team of the Chinese Academy of Sciences (Grant No.GJJSTD20190002), the Chemical Dynamics Research Center Grant No. 21688102), the Strategic Priority Research Program of the Chinese Academy of Sciences (Grant No. XDB17000000), the Natural Science Foundation of Zhejiang Province (LY18B060007), the Chinese Academy of Sciences (GJJSTD20220001) and key Laboratory of Yarn Materials Forming and Composite Processing Technology, Zhejiang Province, China. The authors gratefully acknowledge the Dalian Coherent Light Source (DCLS) for support and assistance. We also thank Dr. Jin Cui and Dr. Shuwen Yu for their help in the characterization of XPS and in-situ FT-IR spectra. This research used resources from the Dalian Coherent Light Source and Shanghai Synchrotron Radiation Facility. We sincerely express our thanks to Dr. Tao Wu from the Dalian University of Technology for his contribution to the DFT calculation.

Keywords: Sulfur Poisoning • Rhodium • Single-Site Catalysts • Olefin hydroformylation • Structure-Activity Relationship

10.1002/anie.202304282

[1] a) Y. Zhang; P. Glarborg, M. P. Andersson, K. Johansen, T. K. Torp, A. D. Jensen, J. M. Christensen, *Appl. Catal. B: Environ.* **2020**, *277*, 119176. b) A. Alarcón. J. Guilera, R. Soto, T. Andreu, *Appl. Catal. B: Environ.*, **2020**, *263*, 118346. c) W. Zhou, W. L. Teo, S. Z. F. Phua, S. Xi, B. Chen, D. Jana, D. Wang, C. Qian, H. Wang, H. Zhang, Y. Zhao, *Small Methods* **2020**, *4*, 1900890.

[2] D. E. Doronkin, T. S. Khan, T. Bligaard, S. Fogel, P. Gabrielsson, S. Dahl, *Appl. Catal. B: Environ.*, **2012**, *117*, 49-58.

[3] C. H. Bartholomew, P. K. Agrawal, J. R. Katzer, In *Advances in Catalysis*, D. D. Eley, H. Pines, P. B. Weisz, Eds. Academic Press, **1982**, *31*, 135-242.

[4] a) Y. Hang, P. Glarborg, M. P. Andersson, K. Johansen, J. M. Christensen, *Appl. Catal. B: Environ*., **2020**, *277*, 119176. b) D. L. Mowery, M. S. Graboski, T. R. Ohno, R. L. McCormick, *Appl. Catal. B: Environ.*, **2010**, *373*, 3969–3980. c) A. Gremminger, P. Lott, M. Merts, M. Casapu, J. D. Grunwaldt, O. Deutschmann, *Appl. Catal. B: Environ.*, **2017**, *218*, 833-843. d) F. Arosio, S. Colussi, G. Groppi, A. Trovarelli, *Catal. Today*, **2006**, *117*, 569-576. e) V. Mesilov, S. Dahlin, S. L. Bergman, S. Xi, J. Han, L. Olsson, L. J. Pettersson, S. L. Bernasek, *Appl. Catal. B: Environ.*, **2021**, *299*, 120626.

[5] S. Cimino, E. M. Cepollaro, L. Lisi, *Appl. Catal. B: Environ.*, **2022**, *317*, 121705.

[6] a) L. S. Escandón, S. Ordóñez, A. Vega, F.V. Díez, *J. Hazard. Mater*, **2008**, *153*, 742–750. b) D. L. Mowery, R. L. McCormick, *Appl. Catal. B: Environ.*, **2001**, *34*, 287–297.

[7] S. Cimino, G. Mancino, L. Lisi, *Appl. Catal. B: Environ.*, **2013**, *138*, 342-352.

[8] P. Lott, M. Eck, D. E. Doronkin, A. Zimina, O. Deutschmann, *Appl. Catal. B: Environ.*, **2020**, *278*, 119244.

[9] S. Gao, L. Wang, H. Li, Z. Liu, G. Shi, J. Peng, B. Wang, W. Wang, K. Cho, *Phys. Chem. Chem. Phy.*, **2021**, *23*, 15010-15019.

[10] a) S. K. Kaiser, Z. P. Chen, D. F. Akl, S. Mitchell, J. Perez-Ramirez, *J., Chem. Rev.*, **2020**, *120*, 11703-11809. b) R. Qin, K. Liu, Q. Wu, N. Zheng, *Chem. Rev.*, **2020**, *120*, 11810-11899. c) M. Babucci, A. Guntida, B. C. Gates, *Chem. Rev.*, **2020**, *120*, 11956-11985. d) H. Y. Zhuo, X. Zhang, J. X. Liang, Q. Yu, J. Li, *Chem. Rev.*, **2020**, *120*, 12315-12341. P. Serna, B. C. Gates, *Accounts Chem. Res.*, **2014**, *47*, 2612-2620.

[11] W. Yang, X. Liu, X. Chen, Y. Cao, S. Cui, L. Jiao, C. Wu, C. Chen, D. Fu, I. D. Gates, Z. Gao, H. L. Jiang, *Adv. Mater.*, **2022**, *34*, 2110123.

[12] a) Q. Yuan, Y. Gu, S. Feng, X. Song, J. Mu, B. Li, X. Li, Y. Cai, M. Jiang, L. Yan, J. Li, Z. Jiang, Y. Wei, Y. Ding, *ACS. Catal.*, **2022**, *12*, 4203-4215. b) S. Feng, J. Mu, X. Lin, X. Song, S. Liu, W. Shi, W. Zhang, G. Wu, J. Yang, W. Dong, X. Yang, J. Li, Z. Jiang, Y. Ding, *Appl. Catal. B: Environ.*, **2023**: *325*, 122318.

[13] R. Franke, D. Selent, A. Börner, *Chem. Rev.*, **2012**, *112*, 5675-5732.

[14] Y. Zhang, S. Torker, M. Sigrist, *J. Am. Chem. Soc.*, **2020**, *142*, 18251-18265.

[15] a) C. Coperet, M. Chabanas, R. Petroff Saint Arroman, *Angew. Chem. Int. Ed.*, **2003**, *42*, 156-181. b) X. Cui, W. Li, P. Ryabchuk, K. Junge, M. Beller, *Nat. Catal.*, **2018**, *1*, 385.

[16] C. Li, L. Yan, L. Lu, *Green Chem.*, **2016**, *18*, 2995-3005.

[17] X. F. Wu, B. Han, K. Ding, Z. Liu, (Eds.). The Chemical Transformations of C1 Compounds. John Wiley & Sons, **2022**.

[18] Q. Sun, Z. Dai, X. Liu, N. Sheng, F. Deng, X. Meng, F. Xiao, *J. Am. Chem. Soc.*, **2015**, *137*, 5204-5209.

[19] D. Evans, G. Yagupsky, G. Wilkinson, *J. Chem. Soc. A Inorg. Phys. Theor.*, **1968**, 2660-2665.

[20] M. Jiang, L. Yan, Y. Ding, Q. Sun, J. Liu, H. Zhu, R. Lin, F. Xiao, Z. Jiang, J. Liu, *J. Mol. Catal. A: Chem.*, **2015**, *404*, 211-217.

[21] R. M. Deshpande, R. V. Chaudhari, *Ind. Eng. Chem. Res.*, **1988**, *27*, 1996-2002.

[22] a) Y. Li, Y. J. Ding, L. W. Lin, H. J. Zhu, H. M. Yin, X. M. Li, L. Yuan, *J. Mol. Catal. A Chem.*, **2009**, *300*, 116-120. b) K. Mukhopadhyay, A. B. Mandale, R. V. Chaudhari, *Chem. Mater.*, **2003**, *15*, 1766-1777.

[23] a) D. Evans, J. A. Osborn, G. Wilkinson, *J. Chem. Soc. A: Inorg., Phys., Theoret.*, **1968**, 3133-3142. b) I. S. Teranishi, *J. Catal.*, **1979**, *58*, 82-94. c) C. Furlani, G. Mattogno, G. Polzonetti, G. Sbrana, G. Valentini, *J. Catal.*, **1985**, *94*, 335-342. d) C. Bianchini, H. M. Lee, A. Meli, F. Vizza, *Organomet.*, **2000**, *19*, 849-853. e) J. L. G. Fierro, J. M. Palacios, F. Tomas, *Surf. Interface Anal.*, **2010**, *13*, 25-32. f) S. S. C. Vander, P. C. J. Kamer, P. W. N. M. Van Leeuwen, J. A. Iggo, B. T. Heaton, *Organomet.*, **2001**, *20*, 430-441. g) S. Feng, X. Lin, X. Song, B. Mei, Y. Ding, *ACS Catal.*, **2021**, *11*, 682-690.

[24] a) M. Arfelli, C. Battistoni, G. Mattogno, D. M. P. Mingos, *J. Electron Spectrosc.*, **1989**, *49*, 273-277. b) H. S. Tao, U. Diebold, N. D. Shinn, T. E. Madey, *Surf. Sci.*, **1994**, *312*, 323-344.

[25] R. S. Clegg, J. E. Hutchison, *Langmuir*, **1996**, *12*, 5239-5243.

[26] V. I. Nefedov, Y. V. Salyn, B. Walther, B. Messbauer, *Inorgan. Chim. Act.*, **1980**, *45*, 103-104.

[27] a) S. Hoste, D. Vondel, G. Kelen, *J. Electron Spectros.*, **1979**, *17*, 191-195. b) W. E. Morgan, W. J. Stec, R. G. Albridge, J. R. Van Wazer, *Inorgan. Chem.*, **1971**, *10*, 926-930. c) NIST X-ray Photoelectron Spectroscopy Database. NIST Standard Reference Database Number 20 **(retrieved [2023]).** d) K. Yasuharu, T. Chisato, S. Ayaka, S. Masatoshi, U. Yoshio, *Appl. Catal. A: General*, **2014**, *475*, 410-419. e) X. Lan, W. Zhang, L. Yan, Y. Ding, X. Han, L. Lin, X. Bao, *J. Phys. Chem. C*, **2009**, *113*, 6589-6530.

[28] M. Garland, P. Pino, *Organomet.* **1991**, *10*, 1693-1704.

[29] G. Liu, R. Volken, M. Garland, *Organomet.*, **1999**, *18*, 3429-3436.

[30] C. Bianchini, H. M. Lee, A. Meli, F. Vizza, *Organomet.*, **2000**, *19*, 849-853.

[31] a) G. Li, Y. Zhang, Q. Li, C. Wang, Y. Yu, B. Zhang, H. Hu, W. Zhang, D. Dai, G. Wu, *Nat. Commun.*, **2020**, *11*, 5449. b) J. Zhou, Y. Zhao, C. S. Hansen, J. Yang, Y. Chang, Y. Yu, G. Cheng, Z. Chen, Z. He, S. Yu, *Nat. Commun.*, **2020**, *11*, 1547. c) Y. Chang, Y. Yu, H. Wang, X. Hu, Q. Li, J. Yang, S. Su, Z. He, Z. Chen, L. Che, *Nat. Commun.*, **2019**, *10*, 1250. d) W. R. Moser, C. J. Papile, D. A. Brannon, R. A. Duwell, S. J. Weininger, *J. Mol. Catal.*, **1987**, *41*, 271-292.

[32] a) E. B. Walczuk, P. Kamer, P. Leeuwen, *Angew. Chem.*, **2003**, *42*, 4665-4669. b) D. Van, M. Boele, F. R. Bregman, P. Kamer, P. V. Leeuwen, K. Goubitz, J. Fraanje, H. Schenk, C. Bo, *J. Am. Chem. Soc.*, **1998**, *120*, 11616-11626. c) N. Sudheesh, J. N. Parmar, R. S. Shukla, *Appl. Catal. A: General*, **2012**, *415*, 124-131.

[33] a) L. R. Mills, R. K. Edjoc, S. A. Rousseaux, *J. Am. Chem. Soc.*, **2021**, *143*, 10422-10428. b) P. Das, P. Chutia, D. K. Dutta, *Chem. Lett.*, **2002**, *31*, 766-767.

10.1002/anie.202304282

WILEY-VCH

RESEARCH ARTICLE

Entry for the Table of Contents

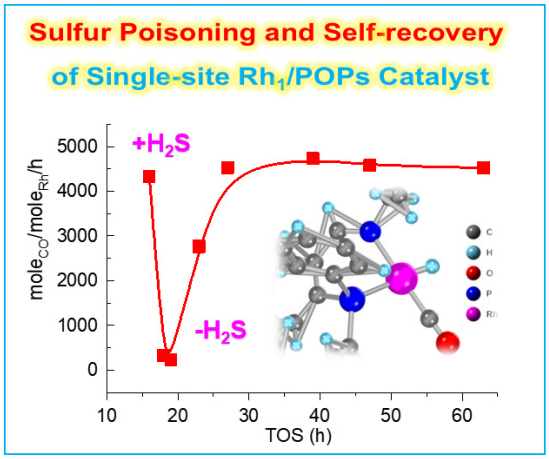

Even at the ppm level, sulfur poisoning and regeneration are challenges for metal nanoparticle catalysts, but little is known about single-metal-site catalysts. Herein, we describe the unique character of single-site catalysts (Rh_1/POPs) that suffer from H_2S poisoning but could self-recover and be regenerated by simply withdrawing the H_2S. The corresponding Rh nanoparticle demonstrated poor activity and could not be regenerated.